REGULAR ARTICLE

A TD-DFT Study on Fluorescent Chemosensor for Fluoride Anion

Based on Dipyrrolyl Derivatives

Cai-Yun Lv, Li-Juan Sun, Bing-Qiang Wang¹, Cai-Yun Zhang, Jian Zhang

School of Chemistry and Material Science, Shanxi Normal University, 041004 Linfen, China Received 2 May 2013; Accepted (in revised version) 6 June 2013

Abstract: Time-dependent density functional theory (TD-DFT) method was used to study the excited-state hydrogen bonds between dipyrrolyl derivatives and fluoride anion (F-). The geometric structures, charge density distribution and electronic spectra of two dipyrrolyl derivatives and their doubly hydrogen-bonded complexes with F- were calculated by the DFT and TD-DFT methods. The intermolecular hydrogen bonds in ground states were proposed to be the main reasons for the gradual spectral shifts in the absorption spectra. The excited-state proton transfer (ESPT) was used to explain well fluorescence emission features of their hydrogen-bonded complexes. Furthermore, the radiationless deactivation via internal conversion (IC), which gives rise to fluorescent quenching of dipyrrolyl derivatives, could be facilitated by the ESPT process.

AMS subject classifications: 92E99

Keywords: Time-dependent density functional theory; Excited-state hydrogen bond; Excited-state proton transfer; Colorimetric chemosensor; Fluorescent chemosensor.

1. Introduction

Hydrogen bonding is a contemporary research interest because of its universal importance in physics, chemistry, biology and other many branches of science [1-4]. Intermolecular hydrogen bonding has been recognized to play a fundamental role in molecular and supramolecular photochemistry [4-9]. Excited-state hydrogen bonds have been investigated

¹ Corresponding author. *Email address*: wangbq2007@163.com. Tel: (86)-357-2051192

experimentally and theoretically in some photophysical and photochemical processes of hydrogen bonding systems [6, 10-18].

Upon photoexcitation of hydrogen-bonded systems, the hydrogen donor and acceptor molecules reorganize due to the significant difference in the charge distribution of different electronic states [5, 7, 17-20]. In a number of cases, these reorganizations can strengthen the intermolecular hydrogen bonding in the electronically excited state and facilitate the radiationless deactivation, i.e. internal conversion (IC) process[6, 10, 21, 22]. This mechanism has been used to explain many photophysical processes, such as fluorescence quenching [8, 10, 23, 24], ultrafast internal conversion [6, 23, 25], etc.

Furthermore, more and more attention has been paid to the role played by hydrogen bond for the design of efficient anion chemosensor. Many neutral organic molecules containing N-H functional groups represent the most commonly seen anion interacting moities. It is noted that a π -system bearing an N-H moiety may be an appropriate candidate for designing anion chemosensors [26-29]. For this kind of receptors, the hydrogen bond-induced π -electron delocalization or basic anion-induced N-H deprotonation serves as the signaling output of the anion-receptor interaction [30, 31]. In recent years, many studies have focused on the mechanism of such processes [4,6, 30, 32].

Recently, pyrrolyl derivatives as anion-binding motif have attracted considerable attention [9]. Pyrrole is an ideal group for the construction of anion receptors. For example, Ghosh and Maiya reported that an easy-to-prepare dipyrrolyl derivative endowed with electron-withdrawing dicyano groups permit the detection of fluoride anion visually and optically [33, 34]. In particular, pyrrole does not contain an intramolecular hydrogen-bonded acceptor that could compete with anion recognition. A pyrrole N-H proton has a lessened dependence on the pH value of the environment. Over the last decades, pyrrole has emerged as an important structural motif that may be used to construct receptor system capable of interacting effectively and selectively with a range of anionic substrates in many instances [33-37]. However, up to now, there have been few theoretical studies on the hydrogen-bonded interactions of pyrrolyl derivatives with anions and photophysical properties of these systems.

In this paper, we report a theoretical study on the isolated dipyrrolypyrazine (DPP) and dipyrrolyldicyanopyrazine (DPDCP) (see **Figure 1**) as fluorescent chemosensors for fluoride anion. In particular, we have focused our attention on the mechanism relating to the gradual spectral shifts and the fluorescence quenching by the hydrogen-bonding interaction between two chemosensors and fluoride anion in both the ground state and the excited state. Furthermore, the dipyrrolyl derivative DPDCP endowed with electron-withdrawing dicyano groups was verified to be more efficient chemosensor for fluoride anion than DPP.

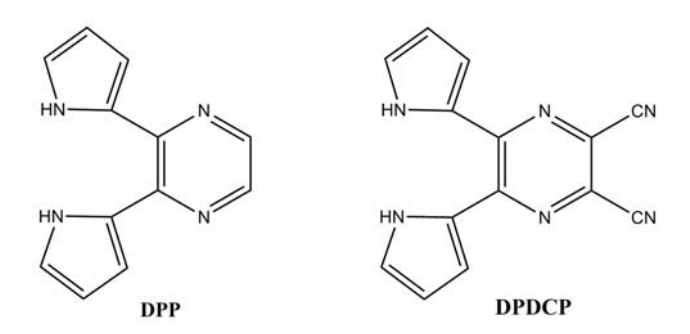


Figure 1: Molecular structures of DPP and DPDCP.

2. Computational Details

The ground state geometric optimizations of the DPP and DPDCP monomers as well as the hydrogen-bonded DPP-F- and DPDCP-F- complexes were performed using density functional theory (DFT) with Becke's three-parameter hybrid exchange function with Lee–Yang–Parr gradient-corrected correlation functional (B3LYP functional). The excited-state electronic structures of all the compounds were calculated using the time-dependent density functional theory (TD-DFT) method employing B3LYP hybrid functional, which has been used widely to investigate the excited-state hydrogen bonds [38, 39]. 6-311++G** basis set was nearly optimal for achieving geometry optimizations and excitation energies in excellent agreement with experimental results [40]. Therefore, 6-311++G** basis set was used in our calculations. No constrains for symmetry, bond lengths, angles or dihedral angles were applied in the geometry optimization calculations. All the local minima were confirmed by no imaginary mode from vibrational analysis calculations.

The solvent effect was considered by using the Polarizable Continuum Model (PCM) model. The ground and excited state geometries were reoptimized at the PCM-B3LYP/6-311++G** and PCM-TD-B3LYP/6-311++G** level, respectively. Absorption spectra were calculated within the non-equilibrium limit, and the emission energies were calculated within the equilibrium limit [41-43]. All the calculations were carried out using Gaussian 09 program package [44].

3. Results and Discussion

3.1 Optimized geometric structures in the ground state

The optimized geometrical structures in the ground state for DPP (1, 2 and 3) and DPDCP

(1-CN, 2-CN and 3-CN) (see **Supporting Information**) were obtained at the B3LYP/6-311++G** level, respectively. These optimized geometrical structures and their relative energies are shown in **Figure SI** and **Table SI** in the Supporting Information. However, upon the addition of a fluoride anion, only one stable hydrogen-bonded structure was obtained for both DPP-F- and DPDCP-F-. The most stable structures of monomers and hydrogen complexes of DPP and DPDCP are shown in **Figure 2**.

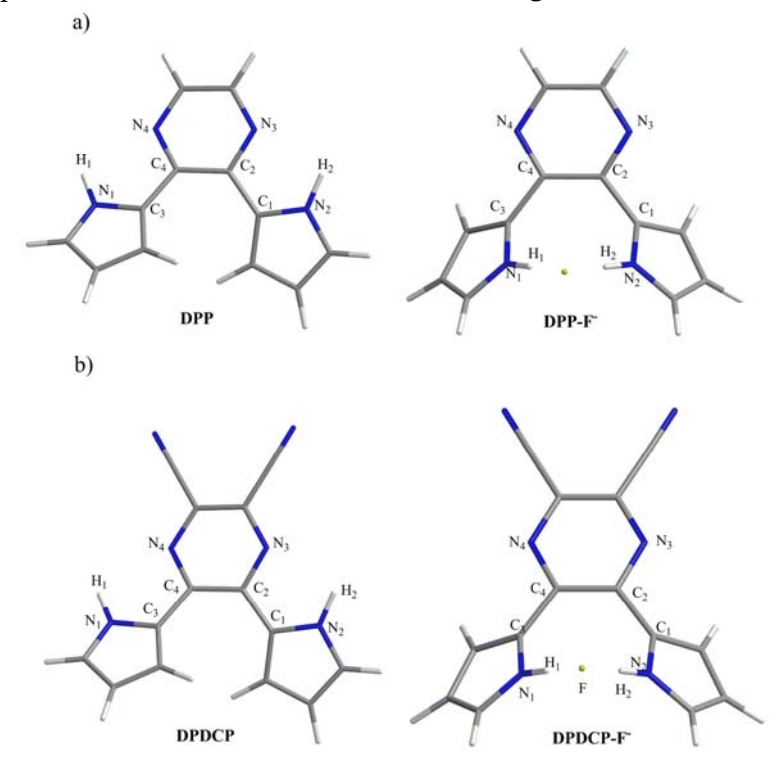


Figure 2: Ground-state geometric structures: a) DPP monomer and DPP-F⁻ complex; b) DPDCP monomer and DPDCP-F⁻ complex.

Some of the most important structural parameters of monomers and hydrogen complexes of DPP and DPDCP are shown in **Table 1**. From **Table 1** and **Figure 2**, one can see that the most stable conformers of DPP and DPDCP have C₂ symmetry constraints. The bond lengths of both the N₁-H₁ and N₂-H₂ are 1.008 Å in the DPP monomer, which are almost equal to 1.009 Å in DPDCP. Two pyrrolyl rings stick out of the pyrazine plane by the angle of 14.6° in DPP and 12.0° in DPDCP, respectively. Introduction of electron withdrawing substituent (-CN) has little effect on the geometrical structures in the ground state.

Table 1: The calculated geometric parameters for monomers DPP and DPDCP and hydrogen-bonded complexes DPP-F- and DPDCP-F- by the DFT and TD-DFT methods at the

B3LYP/6-311++G** level.

			S_0		S ₁				
	DPP	DPP-F	DPDCP	DPDCP-F-	DPP	DPP-F	DPDCP	DPDCP-F-	
Bond									
lengths(Å)									
R(N ₁ ,H ₁)	1.008	1.070	1.009	1.076	1.012	1.490	1.009	1.513	
R(N ₂ ,H ₂)	1.008	1.070	1.009	1.076	1.012	1.014	1.014	1.015	
R(H1,F)		1.478		1.445		1.001		0.999	
$R(H_2, F)$		1.478		1.445		2.064		1.995	
Bond angles(º)									
A(N ₁ ,H ₁ ,F)		174.8		176.1		169.2		168.2	
$A(N_2,H_2,F)$		174.8		176.1		163.3		165.4	
Dihedral angles(º)									
$D_{1^{a}}$	14.6	42.5	12.0	37.9	19.7	64.0	19.0	89.1	
D_2^b	14.6	42.5	12.0	37.9	19.7	88.6	19.0	59.7	

 $[^]aD_1$ is the angle between left pyrrolyl ring and the pyrazine plane. bD_2 is the angle between right pyrrolyl ring and the pyrazine plane.

The structure of DPP-F⁻ complex has a C_s symmetry constraint. Compared with the monomer of DPP, the two bond lengths of N_1 -H₁ and N_2 -H₂ are lengthened by 0.062 Å. Two pyrrolyl rings stick out of the pyrazine plane by the angle of 42.5°. Furthermore, the bond lengths of the two intermolecular hydrogen bonds N_1 -H₁····F-and N_2 -H₂····F-are 1.478 Å.

Like DPP-F⁻, DPDCP-F⁻ complex has also a C_s symmetry constraint. Compared with DPDCP, the bond lengths of N_1 -H₁ and N_2 -H₂ are lengthened by 0.067 Å. Two pyrrolyl rings stick out of the pyrazine plane by the angle of 37.9° .

It should be mentioned that for the DPDCP-F- complex, both the bond lengths of H₁···F- and H₂···F- are shortened by 0.033Å compared to the DPP-F- complex, and the corresponding bond angles N₁-H₁···F- and N₂-H₂···F- were changed from 174.8° to 176.1° compared to the DPP-F- complex. These calculated results indicate the intermolecular hydrogen bonds are strengthened by introducing into two cyano groups in parent molecule DPP. On the other hand, the angles between two pyrrolyl rings and the pyrazine plane

decrease by 4.6°. The differences in strength of the intermolecular hydrogen bonds in the ground state should be responsible for the differences in photophysical properties of complexes [5].

3.2 Absorption spectra

We have calculated the absorption spectra of monomers and complexes of DPP and DPDCP at the TD-DFT/B3LYP/6-311++G** level based on the optimized ground-state geometric structures, and the results are listed in **Table 2**.

Table 2: The absorption spectra (in nm) and oscillator strengths (in the parentheses) for the monomers and complexes of DPP and DPDCP in gas-phase were calculated at the TD-DFT/B3LYP/6-311++G** level. The orbital transitions between orbits and corresponding contributions are also listed.

	DPP	DPP -F	DPDCP	DPDCP -F-
S ₁	384	389	429	470
	(0.107)	(0.090)	(0.108)	(0.130)
	H→L	H→L	H→L+1	H→L
	(+84%)	(+88%)	(+77%)	(+82%)
S ₂	354	374	423	467
	(0.286)	(0.025)	(0.246)	(0.023)
	H→L+1	H-1→L	H→L	H→L+1
	(+85%)	(+95%)	(+82%)	(+65%)
S ₃	316	360	344	410
	(0.081)	(0.188)	(0.119)	(0.129)
	H-1→L	H→L+1	H-1→L+1	H-1→L+1
	(+85%)	(+91%)	(+91%)	(+87%)
HOMO:1	H, LUMO:L.			

For monomer DPP, the absorption maximum can be assigned to the $S0 \rightarrow S2$ transition at 354 nm with oscillator strength of 0.286, and another strong $S0 \rightarrow S1$ absorption peak is at 384 nm with oscillator strength of 0.107. For the hydrogen-bonded DPP-F- complex, the absorption maximum was found to be the $S0 \rightarrow S3$ transition at 360 nm with oscillator strength of 0.188, and another strong $S0 \rightarrow S1$ absorption peak is at 389 nm with oscillator strength of 0.090. This shows that hydrogen bonding interaction between DPP and F- makes little contribution to the absorption bands of DPP.

For monomer DPDCP, there are $S_0 \rightarrow S_1$ and $S_0 \rightarrow S_2$ absorption peaks located at 429 and

423 nm with oscillator strength of 0.108 and 0.246, respectively. As for the hydrogen-bonded DPDCP-F- complex, these two absorption peaks are redshifted by 41 and 44 nm. In addition, the calculated absorption wavelengths for DPDCP and DPDCP-F- are in agreement with experimental results (λ_{abs} (nm): DPDCP,427; DPDCP- F-,469) reported by Ghosh and Maiya [33]. The intermolecular hydrogen bonds between DPDCP and F- cause a considerable red-shift of the electronic transition of DPDCP.

As mentioned in Section 3.1, introduction of electron-withdrawing groups (-CN) gives rise to hydrogen bond strengthening in the ground state. The strengthening of hydrogen bonds should be responsible to the more observable red-shift for electronic spectra of the DPDCP-F- complex than that of DPP-F-. It has been well recognized that the red-shift of electronic spectra in most of hydrogen-bonded systems is attributed to the decrease of the energy gap between the excited and ground states [20, 22, 25]. It is a reasonable deduction that a stronger hydrogen bond can arouse a larger decrease of the energy gap between the excited and ground states. Therefore, the energy gap between the excited and ground states of DPDCP-F- can more significantly decrease than that of DPP-F- because of the stronger intermolecular hydrogen bond in DPDCP-F-. As a consequence, we estimate that DPDCP is more suitable to detect F- than DPP, with more obvious color change upon binding with F- under visual conditions.

3.3 Charge transfer and molecular orbitals (MOs)

In order to gain a deeper insight into the nature of the electronic transition, the frontier molecular orbitals are presented in **Figure 3**.

Much more attention should be paid to electron density distribution of HOMOs, LUMOs, and (LUMO+1)s for monomers and complexes. The electron density distributions in HOMOs are delocalized. However, the electron density distributions of LUMOs and (LUMO+1)s are obviously more localized. With the electronic transitions, intramolecular charge transfer (ICT) can occur from the two pyrrol rings to the pyrazine ring. The hydrogen bonds between NH group on pyrrol ring and F- can be strengthened in excited states due to the decrease of electron density on pyrrol ring with the ICT process. The strengthening of hydrogen bonds in excited states decreases the energy gap between the excited and ground states and causes the red-shift of electronic spectra. ICT process can also be verified by the profile of the difference of total electron density (**Figure SII**) and by the difference of atomic charges in the ground states and excited states (**Table SII**) [45, 46].

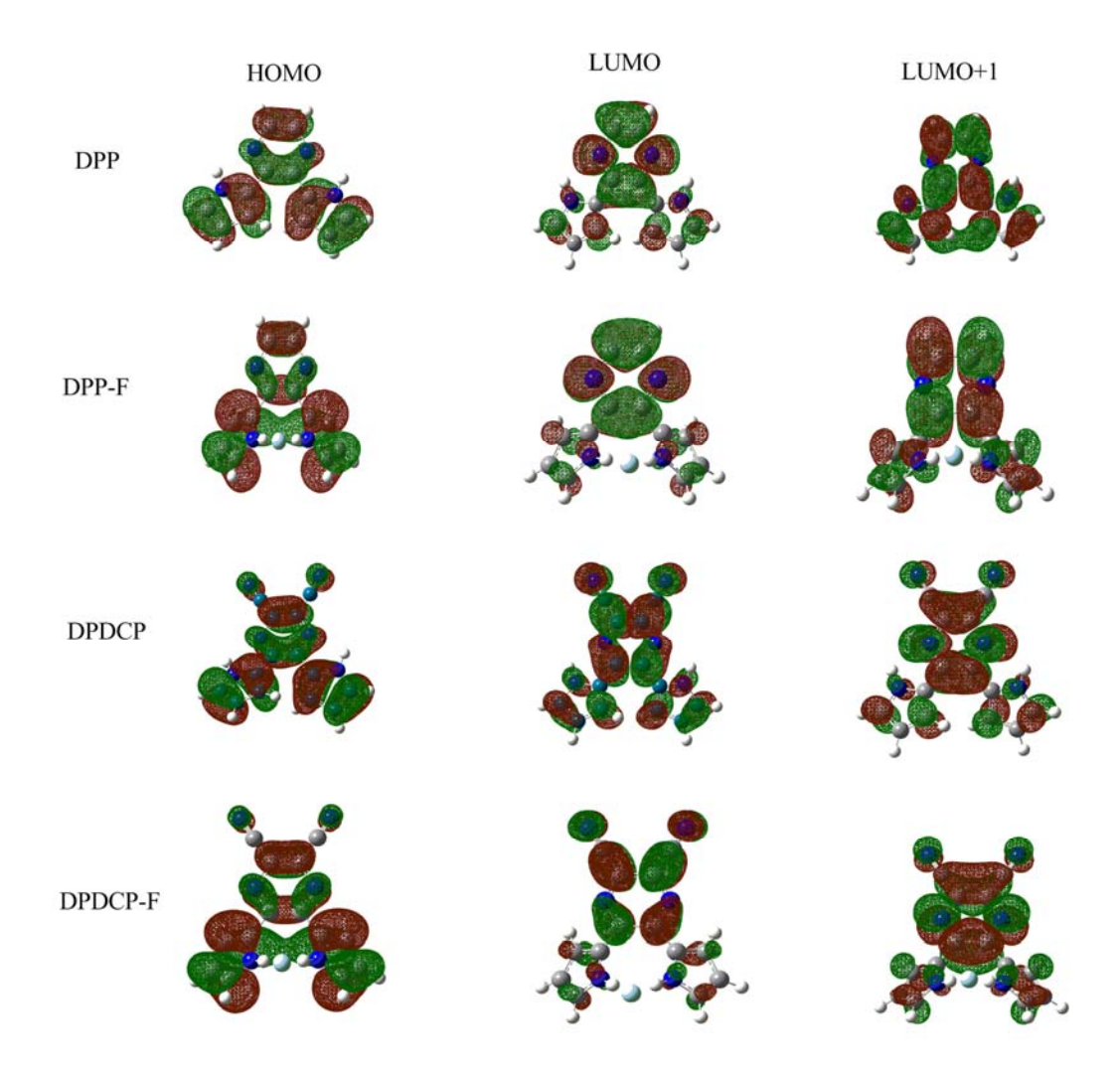


Figure 3: Molecular orbitals of the monomers and complexes of DPP and DPDCP.

As can be seen from **Figure 3** and **Figure SII**, besides the pyrazine ring, the -CN groups accept some of the electron density from the pyrrol rings in DCDCP. Thus, the introduction of electron withdrawing group (-CN) on the DPP could promote ICT and then strengthen the hydrogen bonds in the ground state[5, 7, 45-48]. This is why a more significant red-shift occurs at the DPDCP-F⁻ complex than that at the DPP-F⁻ complex.

3.4 Optimized geometric structures in the first singlet excited state

We have also optimized the first singlet excited-state structures of both the DPP and DPDCP monomers and the hydrogen-bonded complexes at the TD-DFT/B3LYP/6-311++G** level of

theory as shown in **Figure 4**. Some of the most important structural parameters are collected in **Table 1**.

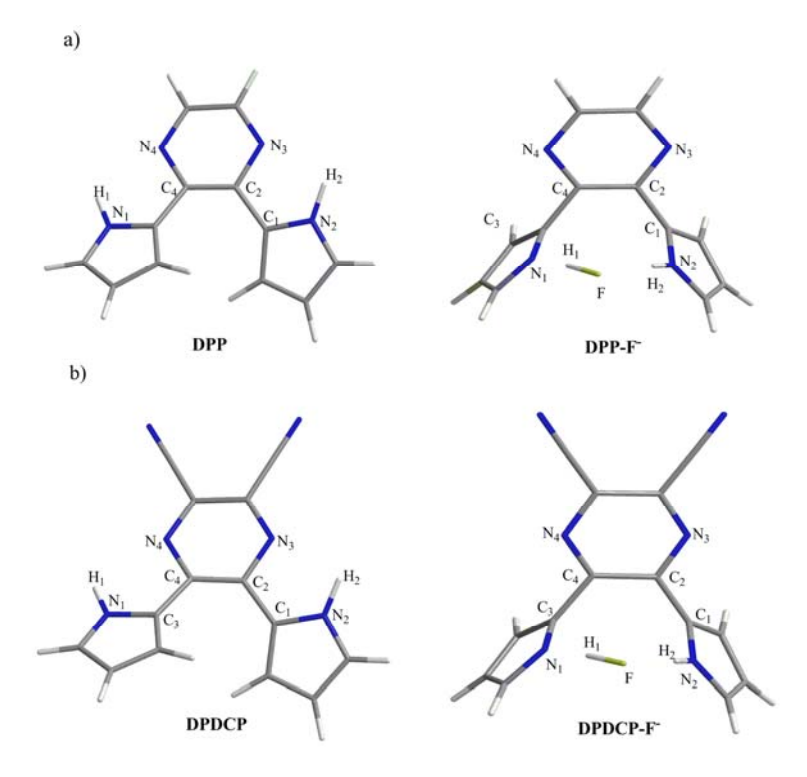


Figure 4: The first excited-state geometric structures: a) DPP monomer and DPP-F- complex; b) DPDCP monomer and DPDCP-F- complex.

In going from the ground state to the excited state, the DPP monomer remains a C_2 symmetry constraint and both the two bond length of N_1 - H_1 and N_2 - H_2 are slightly lengthened by 0.004Å. Two pyrrole rings stick out of the pyrazine plane by the angle of 19.7°. The DPDCP monomer in S_1 state is close to C_2 symmetry. Compared with DPP, introduction of –CN has little effect on the geometrical structure of DPDCP in S_1 state.

For the DPP-F- complex, its C_s symmetry is destroyed after excitation to the S₁ state. Compared with the S₀ state, the bond length of N₁-H₁ is lengthened by 0.420Å, whereas the bond length of N₂-H₂ is shortened by 0.056Å in the S₁ state. The angle between left pyrrolyl ring and the pyrazine plane is 64.0°, and the angle between right pyrrolyl ring and the pyrazine plane is 88.6°. The bond distances of H₁-F and H₂-F are 1.001Å and 2.064Å, respectively. The bond distance of N₁-H₁ is much longer than N-H covalent bond length (1.01Å), and the bond distance of H₁-F is close to H-F covalent bond length (0.92Å). Obviously, ESPT occurs at the DPP-F- complex. As mentioned above, proton transfer can be facilitated by the hydrogen bonding interaction in the electronic excited state [32, 49-51].

As for hydrogen-bonded complex DPDCP-F-, its C_s symmetry is also destroyed after excitation to the S₁ state. The bond length of N₁-H₁ is lengthened by 0.437Å, whereas the bond length of N₂-H₂ is shortened by 0.061Å in the S₁ state. The angle between left pyrrolyl ring and the pyrazine plane is 89.1°, and the angle between right pyrrolyl ring and the pyrazine plane is 59.7°. The bond distance of H₁-F is shortened to 0.999 Å, which is close to H-F covalent bond length (0.92Å) in a free HF molecule. In both DPP-F- and DPDCP-F-, the conformational relaxation of S₁ geometry involves excited state proton transfer from pyrrolyl ring to fluoride anion.

3.5 Fluorescence emission

The emission energies of DPP, DPDCP and the corresponding hydrogen-bonded complexes are calculated by the TD-DFT/B3LYP/6-311++G** method based on the excited-state optimized geometric structures (see **Table 3**).

Table 3: The calculated electronic emission energies (in eV) of S1→S0 transitions for the DPP and DPDCP monomers and the corresponding hydrogen-bonded complexes in gas-phase obtained by TD-DFT/B3LYP/6-311++G** method.

	DPP	DPP-F	DPDCP	DPDCP-F
$S_1 \rightarrow S_0$	2.73	1.36	2.32	0.63

For the hydrogen-bonded complex of DPP, after relaxation of the S_1 excited state, the $S_1 \rightarrow S_0$ transition energy decreases significantly. The calculated emission energies of DPP and DPP-F- are 2.73eV and 1.36eV, respectively. This means that the ESPT process can cause the decrease of the energy gap between the S_1 and S_0 states.

For DPDCP, the calculated emission band of the S₁→S₀ transition is at 535 nm (2.32 eV), which is consistent with the experimental result that DPDCP was found to show fluorescence (λ_{em}(nm):541(0.41))[33]. In DPDCP-F-, the energy gap between the S₁ and S₀ states is significantly lowered to 0.63 eV from 2.32 eV of DPDCP. According to the energy gap law, the probability of internal conversion (IC) between two electronic states is inversely proportional to the energy gap between the two states. With the ESPT process, the energy gap between the S₁ and S₀ states of DPDCP decreases significantly and the radiationless deactivation via IC becomes the main dissipative channel. This causes that the quantum yield of excited-state deactivation via fluorescence is decreased and the fluorescence emission at 541 nm quenches for DPDCP. In other words, the radiationless deactivation via IC can be significantly facilitated by ESPT process. The theoretical result is verified in some photophysical and photochemical processes of hydrogen bonding systems [4, 6, 23, 25, 52].

Since many fluorescent chemosensors can recognize fluoride anion through hydrogen-bonding interactions, the ESPT may play an important role for designing new types of fluorescent chemosensors.

3.6 Solvent effects on the electronic spectra

Solvent effects on the absorption and emission spectra are shown in **Table 4**. As can be seen from **Table 4**, the absorption spectra of these four systems are very sensitive to the CH₂Cl₂ solvent, and large red-shifts of absorption spectra for DPP-F- and DPDCP-F- have been observed from the gas phase to the CH₂Cl₂ solution. In addition, the first absorption band of DPP-F- is noticeably red-shifted by 20 nm for DPP-F- and by 38 nm for DPDCP-F- due to hydrogen bonding in the CH₂Cl₂ solvent. Moreover, in the PCM model with CH₂Cl₂ solvent, the red-shift of the first absorption caused by hydrogen bond in DPDCP-F- was calculated to be 38 nm, which is in a good agreement with 42 nm from experiments [33]. Consequently, although the calculations with the PCM model of solvation systematically underestimated the absolute values of electronic transition energy, they are successful to predict the relative energies of electronic transition, such as the red-shift of absorption spectra by hydrogen bond in DPDCP-F-.

Table 4: The calculated absorption wavelengths (λ abs in nm) and emission energies (in eV) for the DPP and DPDCP monomers and the corresponding hydrogen-bonded complexes in gas phase as well as dichloromethane (CH₂Cl₂) solvent at the TD-DFT/B3LYP/6-311++G** level.

	DPP		DPP-F		DPDCP		DPDCP-F-	
	Gas	CH ₂ Cl ₂	Gas	CH ₂ Cl ₂	Gas	CH ₂ Cl ₂	Gas	CH ₂ Cl ₂
Absorption								
$S_0 \rightarrow S_1$	384	396	389	416	429	496	470	534
Emission								
$S_1 \rightarrow S_0$	2.73	2.45	1.36	0.48	2.32	1.71	0.63	

As shown in **Table 4**, the emission energies are also very sensitive to the CH₂Cl₂ solvent. The emission energies decreased by 0.28 eV for DPP and 0.88 eV for DPP-F⁻ from the gas phase to the solvent, respectively. The emission energy of DPDCP decreased by 0.61 eV from the gas phase to the solvent. It is reasonable to suppose that the emission energy of DPDCP-F⁻ would decrease in CH₂Cl₂ solvent. That means that the conclusion that the

radiationless deactivation via IC can be significantly facilitated by ESPT process for DPDCP-F⁻ is still proper in CH₂Cl₂ solvent.

4. Conclusions

In conclusion, we have calculated the geometric conformations and electronic spectra of the isolated DPP and DPDCP molecules as well as hydrogen-bonded DPP-F- and DPDCP-F- complexes in both the ground state S₀ and the first singlet excited state S₁, respectively.

For DPDCP-F-, the intermolecular hydrogen bonds are strengthened by introducing into two cyano groups in parent molecule DPP. The strengthening of the intermolecular hydrogen bonds gives rise to a more pronounced red-shift for absorption spectra of the DPDCP-F- complex than that of DPP-F-. Thus, DPDCP is more suitable to detect F- than DPP, with more obvious color change upon binding with F- under visual conditions.

After photoexcitation, a considerable ESPT process between pyrrole and F⁻ occurs in both DPDCP-F⁻ and DPP-F⁻, which can significantly lower the energy gap between the S₁ and S₀ states and facilitate the radiationless deactivation of the electronically excited state via internal conversion (IC). As a result, ESPT plays an important role for the fluorescence quenching in DPDCP-F⁻.

References

- [1] D.W. Bolen, G.D. Rose, Structure and energetics of the hydrogen-bonded backbone in protein folding, Annu. Rev. Biochem., 77 (2008), 339-362.
- [2] P. Slavicek, M. Farnik, Photochemistry of hydrogen bonded heterocycles probed by photodissociation experiments and ab initio methods, Phys. Chem. Chem. Phys., 13 (2011), 12123-12137.
- [3] I. Kowalczyk, A.Katrusiak, M. Szafran, Z. Dega-Szafran, Unusual hydrogen-bonding aggregation in 4-amino-1-(2-carboxyethyl)pyridinium bromide hemihydrate, J. Mol. Struct.,1026 (2012), 150-158
- [4] S. Perun, A.L. Sobolewski, W. Domcke, Role of electron-driven proton-transfer processes in the excited-state deactivation of the adenine-thymine base Pair, J. Phys. Chem. A, 110 (2006), 9031-9038.
- [5] Y.F. Liu, D.P. Yang, D.H. Shi, J.F. Sun, A TD-DFT study on the hydrogen bonding of three esculetin complexes in electronically excited states: strengthening and weakening, J. Comput. Chem., 32 (2011), 3475-3484.
- [6] G.J. Zhao, K.L. Han, Ultrafast hydrogen bond strengthening of the photoexcited fluorenone in alcohols for facilitating the fluorescence quenching, J. Phys. Chem. A, 111 (2007), 9218-9223.
- [7] S.G. Ramesh, S. Re, J.T. Hynes, Charge transfer and OH vibrational frequency red shifts in nitrate–water clusters, J. Phys. Chem. A, 112 (2008), 3391-3398.
- [8] Y.H. Liu, G.J. Zhao, G.Y. Li, K.L. Han, Fluorescence quenching phenomena facilitated by excited-state hydrogen bond strengthening for fluorenone derivatives in alcohols, J. Photochem. Photobiol. A, 209

- (2010), 181-185.
- [9] J.L. Atwood, J.W. Steed, Encyclopedia of Supramolecular Chemistry, Marcel Dekker, New York, 2004.
- [10] G.J. Zhao, J.Y. Liu, L.C. Zhou, K.L. Han, Site-selective photoinduced electron transfer from alcoholic solvents to the chromophore facilitated by hydrogen bonding: a new fluorescence quenching mechanism, J. Phys. Chem. B, 111 (2007), 8940-8945.
- [11] Y.H. Liu, M.S. Mehata, Excited-state proton transfer via hydrogen-bonded acetic acid (AcOH) wire for 6-Hydroxyquinoline, J. Phys. Chem. A, 115 (2010), 19-24.
- [12] J. Lv, D. Yang, A DFT/TDDFT study of hydrogen bonding interactions between resorufin anion and water molecules in the excited state, Comput. Theor. Chem., 970 (2011), 6-14.
- [13] G.J. Zhao, B.H. Northrop, K.L. Han, P.J. Stang, The effect of intermolecular hydrogen bonding on the fluorescence of a bimetallic Platinum complex, J. Phys. Chem. A, 114 (2010), 9007-9013.
- [14] Y. Liu, Y. Yang, K. Jiang, D. Shi, J. Sun, Excited-state N–H***S hydrogen bond between indole and dimethyl sulfide: time-dependent density functional theory study, Phys. Chem. Chem. Phys., 13 (2011), 15299-15304.
- [15] P. Fita, M. Fedoseeva, E. Vauthey, Hydrogen-bond-assisted excited-State deactivation at liquid/water interfaces, Langmuir, 27 (2011), 4645-4652.
- [16] B. Valeur, Molecular fluorescence: principles and applications, Wiley-VCH, Weinheim, 2001.
- [17] G.J. Zhao, K.L. Han, Early time hydrogen-bonding dynamics of photoexcited Coumarin 102 in hydrogen-donating solvents: theoretical Study. J. Phys. Chem. A, 111 (2007), 2469-2474.
- [18] G.J. Zhao, K.L. Han, Hydrogen bonding and transfer in the excited state, John Wiley & Sons Ltd, Chichester, UK, 2010.
- [19] J.T. Hynes, T.H. Tran-Thi, G. Granucci, Intermolecular photochemical proton transfer in solution: new insights and perspectives, J. Photochem. Photobiol. A, 154 (2002), 3-11.
- [20] G.J. Zhao, K.L. Han, Hydrogen bonding in the electronic excited state, Acc. Chem. Res., 45 (2012), 404–413.
- [21] G.J. Zhao, K.L. Han, Site-specific solvation of the photoexcited protochlorophyllide a in Methanol: formation of the hydrogen-bonded intermediate state induced by hydrogen-bond strengthening, Biophys. J., 94 (2008), 38-46.
- [22] G.J. Zhao, K.L. Han, Effects of hydrogen bonding on tuning photochemistry: concerted hydrogen-bond strengthening and weakening, ChemPhysChem, 9 (2008), 1842-1846.
- [23] P.S. Murthy, Molecular handshake: recognition through weak noncovalent interactions, J. Chem. Educ., 83 (2006), 1010-1025.
- [24] A. Morimoito, T. Yatsuhashi, T. Shimada, L. Biczók, D.A. Tryk, H. Inoue, Radiationless deactivation of an intramolecular charge transfer excited state through hydrogen bonding: effect of molecular structure and hard–soft anionic character in the excited State, J. Phys. Chem. A, 105 (2001), 10488-10496.
- [25] G.J. Zhao, K.L. Han, Role of intramolecular and intermolecular hydrogen bonding in both singlet and

- triplet excited states of aminofluorenones on Internal Conversion, Intersystem Crossing, and Twisted Intramolecular Charge Transfer, J. Phys. Chem. A, 113 (2009), 14329-14335.
- [26] C. Caltagirone, P.A. Gale, Fluorescent detection of phosphate anion by a highly selective chemosensor in water, Chem. Soc. Rev., 38 (2009), 520-563.
- [27] P.A. Gale, S.E. García-Garrido, J. Garric, Anion receptors based on organic frameworks: highlights from 2005 and 2006, Chem. Soc. Rev., 37 (2008) 151-190.
- [28] P.A. Gale, Anion receptor chemistry: highlights from 2008 and 2009, Chem. Soc. Rev., 39 (2010), 3746-3771.
- [29] P.A. Gale, R. Quesada, Anion coordination and anion-templated assembly: highlights from 2002 to 2004, Coord. Chem. Rev., 250 (2006), 3219-3244.
- [30] F. Zapata, A. Caballero, A. Tárraga, P. Molina, Ferrocene-substituted Nitrogen-rich ring systems as multichannel molecular chemosensors for anions in aqueous environment, J. Org. Chem., 75 (2009), 162-169.
- [31] P.T. Chou, W.S. Yu, Y.C. Chen, C.Y. Wei, S.S. Martinez, Ground-state reverse double proton transfer of 7-Azaindole, J. Am. Chem. Soc., 120 (1998), 12927-12934.
- [32] G.Y. Li, G.J. Zhao, Y.H. Liu, K.L. Han, G.Z. He, TD-DFT study on the sensing mechanism of a fluorescent chemosensor for fluoride: excited-state proton transfer, J. Comput. Chem., 31 (2010), 1759-1765.
- [33] T.Ghosh, B.G. Maiya, Visual sensing of fluoride ions by dipyrrolyl derivatives bearing electron-withdrawing groups, J. Chem. Sci., 116 (2004), 17-20.
- [34] T.Ghosh, B.G. Maiya, Fluoride ion receptors based on dipyrrolyl derivatives bearing electron-withdrawing groups: synthesis, optical and electrochemical sensing, and computational studies, J. Phys. Chem. A, 108 (2004), 11249-11259.
- [35] J. Wu, A. Zhong, H. Yan, G. Dai, H. Chen, H. Liang, Study on the nature of interaction of pyrrole with various hydrides, Chem. Phys., 386 (2011), 45-49.
- [36] Z. Yang, K. Zhang, F. Gong, S. Li, J. Chen, J.S. Ma, L.N. Sobenina, A.I. Mikhaleva, B.A. Trofimov, G. Yang, A highly selective fluorescent sensor for fluoride anion based on pyrazole derivative: naked eye "no–yes" detection, J. Photochem. Photobiol. A, 217 (2011), 29-34.
- [37] N.G. Giri, S.M.S. Chauhan, Spectroscopic and spectrometric studies of anion recognition with calix[4]pyrroles in different reaction conditions, Spectrochim. Acta Part A, 74 (2009), 297-304.
- [38] R.K. Chen, G.J. Zhao, X.C. Yang, J. Xiao, J.F. Liu, H.N. Tian, G. Yan, X.E. Liu, K.L. Han, M.T. Sun, L.C. Sun, Photoinduced intramolecular charge-transfer state in thiophene-π-conjugated donor–acceptor molecules, J. Mol. Struct., 876 (2008), 102-109.
- [39]G.J. Zhao, B.H. Northrop, P.J. Stang, K.L. Han, Photophysical Properties of Coordination-Driven Self-Assembled Metallosupramolecular Rhomboids: Experimental and Theoretical Investigations, J. Phys. Chem. A, 114 (2010), 3418-3422.
- [40] S. Rafiq, R. Yadav, P. Sen, Femtosecond excited-state dynamics of 4-Nitrophenyl pyrrolidinemethanol:

- evidence of twisted intramolecular charge transfer and intersystem crossing involving the Nitro group, J. Phys. Chem. A, 115 (2011), 8335-8343.
- [41] C. Adamo, D. Jacquemin, The calculations of excited-state properties with Time-Dependent Density Functional Theory, Chem. Soc. Rev., 42 (2013), 845-856
- [42] R.F. Jin, J.P. Zhang, L.Z. Hao, Theoretical study of the excited-state intramolecular proton transfer and rotamerism in 2,5-bis(2-hydroxyphenyl)-1,3,4-oxadiazole, Theor. Chem. Acc., 126 (2010), 351-360.
- [43] D. Jacquemin, J. Preat, Theoretical investigation of substituted anthraquinone dyes, J. Chem. Phys., 121 (2004), 1736-1743.
- [44] M.J. Frisch, G.W. Trucks, H.B. Schlegel, G.E. Scuseria, M.A. Robb, J.R. Cheeseman, G. Scalmani, V. Barone, B. Mennucci, G.A. Petersson, H. Nakatsuji, M. Caricato, X. Li, H.P. Hratchian, A.F. Izmaylov, J. Bloino, G. Zheng, J.L. Sonnenberg, M. Hada, M. Ehara, K. Toyota, R. Fukuda, J. Hasegawa, M. Ishida, T. Nakajima, Y. Honda, O. Kitao, H. Nakai, T. Vreven, J. A. Montgomery, Jr., J. E. Peralta, F. Ogliaro, M. Bearpark, J.J. Heyd, E. Brothers, K.N. Kudin, V.N. Staroverov, T. Keith, R. Kobayashi, J. Normand, K. Raghavachari, A. Rendell, J.C. Burant, S.S. Iyengar, J. Tomasi, M. Cossi, N. Rega, J.M. Millam, M. Klene, J.E. Knox, J.B. Cross, V. Bakken, C. Adamo, J. Jaramillo, R. Gomperts, R.E. Stratmann, O. Yazyev, A.J. Austin, R. Cammi, C. Pomelli, J.W. Ochterski, R.L. Martin, K. Morokuma, V.G. Zakrzewski, G.A. Voth, P. Salvador, J.J. Dannenberg, S. Dapprich, A.D. Daniels, O. Farkas, J.B. Foresman, J.V. Ortiz, J. Cioslowski, and D.J. Fox, Gaussian 09, Revision C.01, Gaussian Inc., Wallingford CT, 2010.
- [45] Y.S. Xue, Y. Liu, L. An, L. Zhang, Y.M. Yuan, J. Mou, L. Liu, Y.G. Zheng, Electronic structures and spectra of quinoline chalcones: DFT and TDDFT-PCM investigation, Comput. Theor. Chem., 965 (2011), 146-153.
- [46] C.A. Kenfack, A.S. Klymchenko, G. Duportail, A. Burger, Y. Mely, Ab initio study of the solvent H-bonding effect on ESIPT reaction and electronic transitions of 3-hydroxychromone derivatives, Phys. Chem. Chem. Phys., 14 (2012), 8910-8918.
- [47] Z.Y. Tu, M.L. Jing, J.Ch. Fu, J.M. Yuan, Shi. Wu, Q.W. Teng, Electronic structures and spectroscopy of sulfonated oligo(aryl ether ketones), Comput. Theor. Chem., 986 (2012), 1-5.
- [48] C.J. John, T.S. Xavier, G. Lukose, I.H. Joe, Electronic absorption and vibrational spectra and nonlinear optical properties of L-valinium succinate, Spectrochim. Acta Part A, 85 (2012), 66-73.
- [49] B. Liu, H. Tian, A ratiometric fluorescent chemosensor for fluoride ions based on a proton transfer signaling mechanism, J. Mater. Chem., 15 (2005), 2681-2686.
- [50] Z. Li, J.P. Zhang, An efficient theoretical study on host–guest interactions of a fluoride chemosensor with F⁻, Cl⁻ and Br⁻.Chem. Phys., 331 (2006), 159-163.
- [51] X.J. Peng, Y.K. Wu, J.L. Fan, M.Z. Tian, K.L Han, Colorimetric and ratiometric fluorescence sensing of fluoride: tuning selectivity in proton transfer. J. Org. Chem., 70 (2005), 10524-10531.
- [52] R. Englman, J. Jortner, The energy gap law for radiationless transitions in large molecules, Mol. Phys., 18 (1970), 145-164.